# Performance Analysis and Mitigation Method for I/Q Imbalance-Impaired Time Reversal-based Indoor Positioning Systems

Trung-Hien Nguyen[1], Sidney Golstein[1], Jérôme Louveaux[2], Philippe De Doncker[1], and François Horlin[1]
[1]OPERA department, Université libre de Bruxelles (ULB), 1050 Brussels, Belgium
[2]ICTEAM institute, Université catholique de Louvain (UCL), 1348 Louvain-la-Neuve, Belgium
Email: trung-hien.nguyen@ulb.ac.be

***Abstract*—Time reversal-based indoor positioning system (TRIPS) is a promising technology for the centimeter-accuracy indoor positioning, since it exploits the rich multipath propagation in indoor environments as a specific signature for each location. In TRIPS, a database is first constructed via channel probing. Well-calibrated devices are usually assumed in this process, i.e., no hardware impairments. However, a low cost terminal to be located, whose typical impairment is the I/Q imbalance (IQI) at the front-end transmitter, can significantly influence the TRIPS performance. More specifically, IQI creates an interference image of the signal that reduces the metric value used in TRIPS and hence decreases the localization accuracy. In this paper, we analytically investigate the impact of the IQI on the metric of TRIPS. A closed-form approximation of the localization metric inherent to the IQI is derived. In order to improve the TRIPS performance, an effective IQI mitigation method is proposed. Numerical simulations are carried out to validate the derived analytical expression under the IQI impact and the proposed compensation method.**

***Index terms*—** Indoor positioning system, time reversal, I/Q imbalance, OFDM.

## I. Introduction

A high accuracy indoor positioning system (IPS) is required to increase the quality of location-based information services, such as advertisement in smart markets, tourist guidance in museums, etc. Compared to the received signal strength (RSS)-based IPS, the channel impulse response (CIR)-based IPS can provide the localization accuracy in the order of tens of centimeters, i.e., fine-grained indoor fingerprinting system (FIFS) [1], due to a better resistance to the non-line-of-sight (NLOS) condition. In order to better integrate IPS into emerging Wi-Fi systems, which is based on orthogonal frequency division multiplexing (OFDM) modulation, i.e., 802.11ac/ax, the channel frequency response (CFR) has recently been used in the IPS [2]. In combination with the time reversal (TR) technique, the CFR-based IPS can provide an accuracy of 10 cm within a $0.9 \times 1$ m considered area of a room.

The time reversal-based indoor positioning system (TRIPS) is composed of two stages: (i) offline database construction consisting of estimated CIR (or CFR) w.r.t. the logical positions of an area and (ii) online position estimation based on the correlation between the estimated CIR (or CFR) of a device to be located and the ones in the database. In order to reduce the cost of the user terminal (UT), the access point (AP) stores the CIR database for the localization. The reference terminal used in the first localization stage can generally assume to be hardware-impairment-free or well-calibrated. Unfortunately, it is not the case for the UT to be located. The I/Q imbalance (IQI), which represents the imbalance between the in-phase (I) and the quadrature (Q) branches in the up-down complex frequency conversion by the sinusoidal oscillators, is one of the major impairments in wireless systems. Compared to the ideal case ($90^\circ$ phase difference and equal amplitudes between I and Q branches), the mismatch between the I and Q branches causes the IQI. The IQI and its influence on the wireless systems have been well investigated in the literature, i.e., [3] and references therein. Recently, we have investigated the IQI impact on the TRIPS performance in [4], however, only by numerical characterization.

In this paper, we analytically study the IQI impact on the TRIPS system and propose a method to mitigate the IQI. More specifically, our contributions are of three-fold:

- Derivation of a closed-form expression of the localization metric under the IQI impact.
- Development of a simple and efficient IQI compensation method to improve the TRIPS performance.
- Numerical validation of the derived expression and the proposed IQI compensation method.

*Notation*: the underlined low-case and upper-case letters represent the column vectors of the time-domain and frequency-domain variables, respectively, the double-underlined upper-case letter represents a matrix; $\underline{\underline{I}}_Q$ is the $Q \times Q$ identity matrix and $\underline{\underline{J}}_Q$ is the $Q \times Q$ anti-diagonal identity matrix, i.e., the first row of $\underline{\underline{I}}_Q$ is the $Q$-th row of $\underline{\underline{J}}_Q$, the second row of $\underline{\underline{I}}_Q$ is the $(Q-1)$-th row of $\underline{\underline{J}}_Q$ and so on; $\underline{\underline{\Lambda}}_X$ is the diagonal matrix

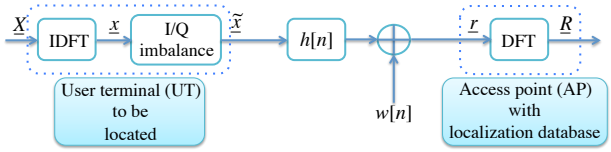


Fig. 1. A time reversal based positioning system (TRIPS) with I/Q imbalance at the transmitter (user terminal).

whose diagonal entries are elements of the vector $\underline{X}$; $||\cdot||_2$, $(\cdot)^*$, $(\cdot)^H$, $(\cdot)^T$, $\mathbb{E}[\cdot]$, $\mathrm{Cov}[\cdot]$ and $\mathrm{tr}\{\cdot\}$ are the Euclidean norm, complex conjugate, Hermitian transpose, transpose, statistical expectation, co-variance and trace operators, respectively; $\Re$ and $\Im$ are the real and imaginary part operators, respectively.

## II. IQI and Its Impact on Channel Estimation

We consider the scenario, where the UT sends a request to the AP to identify its location (Fig. 1). In the indoor environment, the widely-used Wi-Fi technology is based on OFDM modulation, which facilitates the estimate of CFR. In our case, a frequency-domain pilot symbol $\underline{X}$ of $Q$ subcarriers is used to form a repetitive time-domain OFDM probing frame $\underline{x}$ by using inverse discrete Fourier transform (IDFT) of size $Q$, before being sent to the AP. The frequency-domain sequence $\underline{X}$ in the channel probing phase is constructed by a known uniformly distributed sequence of the binary-phase-shift-keying (BPSK) modulation, i.e., $\{\pm 1\}$, and of variance $\sigma_X^2 = 1$. However, the UT front-end sufferring from IQI leads to the modified transmitted signal $\underline{\tilde{x}}$ as follows: $\underline{\tilde{x}} = \mu \cdot \underline{x} + \nu \cdot \underline{x}^*$, in which $\mu$ and $\nu$ are the coefficients dependent on the gain imbalance $\varepsilon$ and the phase imbalance $\theta$ [5]

$$\mu = \left(1 + \varepsilon \cdot \mathrm{e}^{j\theta}\right)/2 \quad \text{and} \quad \nu = \left(1 - \varepsilon \cdot \mathrm{e}^{-\mathrm{j}\theta}\right)/2. \quad (1)$$

After propagation through the channel and addition of a circularly complex white Gaussian noise (AWGN), the frequency-domain received signal can equivalently be written as: $\underline{R} = \left(\mu \cdot \underline{\underline{\Lambda}}_X + \nu \cdot \underline{\underline{\Lambda}}_{\widetilde{X}}\right) \cdot \underline{H} + \underline{W}$, where $\underline{\widetilde{X}} = \underline{\underline{J}}_Q \cdot \underline{X}^*$ is the flipped image version of $\underline{X}$, $\underline{H}$ is the CFR and $\underline{W}$ is the frequency-domain noise vector of variance $\mathbb{E}[|W_q|^2] = \sigma_W^2$. Assuming that $\underline{X}$ is known at the receiver, the estimated CFR is given by

$$\underline{\widehat{G}} = \left(\mu \cdot \underline{\underline{I}}_Q + \nu \cdot \underline{\underline{\Lambda}}_Z\right) \cdot \underline{H} + \underline{\underline{\Lambda}}_X^{-1} \cdot \underline{W}, \quad (2)$$

where vector $\underline{Z}$ stacks elements $Z_q$ defined as the ratio between the frequency-image of $X_q$ and the known symbol $X_q$ as follows

$$Z_q := \begin{cases} 1, & \text{for} \quad q = 0 \\ \dfrac{X_{Q-q}^*}{X_q}, & \text{for} \quad q = 1, ..., Q-1 \end{cases} \quad (3)$$

It can be seen that without IQI, i.e., $\mu = 1$ and $\nu = 0$, the estimated CFR logically reduces to $\underline{\widehat{H}} = \underline{\underline{\Lambda}}_X^{-1} \cdot \underline{R} = \underline{H} + \underline{\underline{\Lambda}}_X^{-1} \cdot \underline{W}$. Without compensation for the IQI, the estimated CFR is modified by an independent term that depends on the pilot sequence and on the image of the CFR and its consequence in TRIPS is studied in Section III.

## III. TRIPS Operation and Metric

We study the indoor localization problem, in which the AP is located in an arbitrarily known location, whereas the position of the IQI-impaired UT needs to be identified. In the TRIPS system, in the first phase, we need to build offline a database that maps the physical geographical locations to the logical locations in the CFR space. After that, the CFR between the UT and the AP is estimated online based on the known sequence. Finally, the estimated CFR is compared to CFRs in the database and the one with the highest cross-correlation gives the information of the UT position. It is worth noticing that compared to the capacity of the current storage devices, the size of the fingerprinting database is relatively small. As an example, only 4.2 MBytes are required to store the database for a room of size $5.4 \times 3.1$ m [2].

### A. Localization Metric

Based on the knowledge of the channel probing sequence at the receiver, the CFR can efficiently be estimated based on (2). In this paper, we use the frequency domain expression of the TR resonating strength in [2] as the localization metric to estimate the position of UT. To facilitate the subsequent derivation of the localization metric in the presence of the IQI, we assume that the time/frequency synchronization is perfect at the receiver and the localization metric is defined as follows [6]

$$\Psi_m := \left| \frac{\underline{H_m}^H \cdot \underline{\widehat{G}}}{\|\underline{H_m}\|_2 \cdot \left\|\underline{\widehat{G}}\right\|_2} \right|^2, \quad (4)$$

where $\underline{H_m}$ denotes the CFR at the logical position $m$ in the database. The logical position $\hat{m}$ corresponding to $\hat{m} = \arg\max_m \Psi_m$ is then transformed to the geographical information in order to identify the location of the UT. Note that, the interested readers can refer to [2], [4] for the synchronization in TRIPS.

As mentioned in our previous work [4], $\Psi_m$ takes values in the range $[0, 1]$. In the absence of the IQI, $\Psi_m$ is close to 1, when the estimated CFR between the AP and the UT matches the one represented to the position $m$ in the database. However, in the presence of the IQI, the localization metric reduces, resulting in a high failure ratio of the positioning [4]. We will derive in the next Section a closed-form expression of the localization metric.

### B. Localization Metric Analysis under the IQI Impact

Assuming that the considered position of the UT associated with the CFR $\widehat{\underline{G}}$ is matched with the desired position of the CFR $\underline{H}_m$ in the database, ignoring the index $m$ for sake of simplicity, we need to compute the following localization metric

$$\Psi = \mathbb{E}_{H,W}\left[\left|\frac{\underline{H}^H \cdot \widehat{\underline{G}}}{\|\underline{H}\|_2 \cdot \left\|\widehat{\underline{G}}\right\|_2}\right|^2\right] \simeq \frac{\mathbb{E}_{H,W}\left[\left|\underline{H}^H \cdot \widehat{\underline{G}}\right|^2\right]}{\mathbb{E}_{H,W}\left[\|\underline{H}\|_2^2 \cdot \left\|\widehat{\underline{G}}\right\|_2^2\right]} \tag{5}$$

The approximation in (5) is made possible using the first-order Taylor approximation of the expectation of a ratio. Based on the derivation in Appendix A, we obtain the closed-form approximation of the localization metric as follows

$$\Psi \simeq \frac{\sum_{p=0}^{Q-1}\sum_{q=0}^{Q-1}(\mu+\nu Z_p)(\mu+\nu Z_q)^* \Theta_{pq} + Q\cdot\sigma_W^2}{\sum_{p=0}^{Q-1}\sum_{q=0}^{Q-1}|\mu+\nu Z_q|^2\Theta_{pq} + Q^2\cdot\sigma_W^2} \tag{6}$$

where $\Theta_{pq} := 1 + |\rho_{q-p}|^2$, $\rho_{q-p}$ is the correlation between the $p$-th and $q$-th CFR components (derived in Appendix B).

- *At high SNRs*: $\sigma_W^2$ is close to 0, the localization metric $\Psi_{high}$ converges to the following expression

$$\Psi_{high} \simeq \frac{\sum_{p=0}^{Q-1}\sum_{q=0}^{Q-1}(\mu+\nu Z_p)(\mu+\nu Z_q)^* \Theta_{pq}}{\sum_{p=0}^{Q-1}\sum_{q=0}^{Q-1}|\mu+\nu Z_q|^2\Theta_{pq}} \tag{7}$$

It can be observed that in the absence of the IQI, $\Psi_{high} = 1$. In the presence of the IQI, $\Psi_{high}$ also represents the computable reduction of the localization metric, which is useful to predict the focusing gain reduction in TRIPS.

- *At low SNRs*: depending on the number of subcarriers $Q$, the contribution of the first summation term or the second noise-dependent term of both numerator and denominator of (3) becomes more dominant. However, at very low SNRs, the noise-dependent term in (3) becomes more dominant, so that the localization metric at low SNRs, $\Psi_{low}$, is inversely proportional to the number of subcarriers, i.e., $\Psi_{low} \simeq 1/Q$.

## IV. IQI Compensation in TRIPS

### A. Previous Studies

A lot of studies on IQI compensation have been reported for the communication systems in the literature. For example, the authors in [3] reported on an expectation-maximization-based IQI compensation algorithm that relies on the preambles of IEEE 802.11a Wi-Fi technology. However, the algorithm considers the compensation of receiver IQI. The authors in [7] proposed an IQI compensation algorithm based on the minimization of so-called channel residual energy. The algorithm can estimate either transmitter or receiver IQI, at a cost of a high computational complexity because the algorithm relies on the inversion of large-size matrix. Although the aforementioned IQI compensation algorithms can be applied in our case, we rather design a simple pilot structure that enables us to quickly estimate the CFR used in the TRIPS.

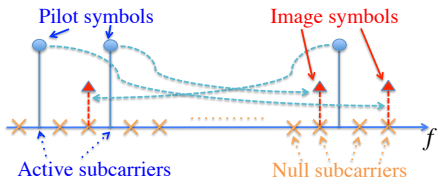


Fig. 2. Examples of pilot symbols design to estimate the IQI.

### B. Pilot Design and IQI Compensation

Before describing the design of pilot symbols $\underline{X}$, we first represent the received symbols in another form as: $\underline{R} = \mu \cdot \underline{\underline{\Lambda}}_H \left(\underline{X} + \alpha\underline{\widetilde{X}}\right) + \underline{W}$, where $\alpha := \nu/\mu$. Defining $\underline{\widetilde{H}} := \mu \cdot \underline{H}$, the received symbols can further be rewritten as: $\underline{R} = \underline{\underline{\Lambda}}_{\widetilde{H}} \left(\underline{X} + \alpha\underline{\widetilde{X}}\right) + \underline{W}$. It can be observed that besides the additive noise $\underline{W}$, the weighted frequency-image symbols $\underline{\widetilde{X}}$ make the CFR estimation inaccurate. We propose to design the pilot symbols such that the pilot-image subcarriers do not overlap with the active pilot subcarriers, i.e., $\underline{\widetilde{X}}$ do not contribute to subcarriers bearing $\underline{X}$. To do so, an asymmetrical pilot symbols allocation (compared to the central frequency) is carried out. It is made possible by progressively assigning the pilot symbols to subcarrier indexes with a step such that the total number of subcarriers $Q$ is not divisible to the index step. As $Q$ is usually a power of 2, to maximize the number of active subcarriers, the increasing index step is chosen to be 3. For example, when $Q = 512$, we set the active subcarriers indexes to be $\{4, 7, ..., 508\}$, the image symbols inherent to the IQI appear at respective subcarriers indexes $\{510, 507, ..., 6\}$ that do not overlap with the active ones. Fig. 2 illustrates the pilot symbols assigment and the associated position of image symbols.

We define $\mathcal{P}$ and $\overline{\mathcal{P}}$ as subsets stacking active and inactive (zero-symbol) subcarriers indexes, respectively. To facilitate notations, the selected symbols of a vector at subset indexes are presented as ones in a new vector with subscript named by the subset, i.e., the received active pilot symbols $\underline{R}_{\mathcal{P}}$. Thanks to the proposed pilot design, the weighted CFR can easily be calculated as

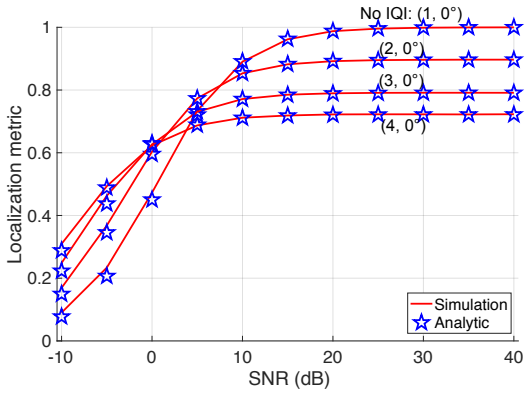


Fig. 3. Localization metric versus SNR for different gain imbalances. The couple $(\varepsilon, \theta)$ is noticed on each curve.

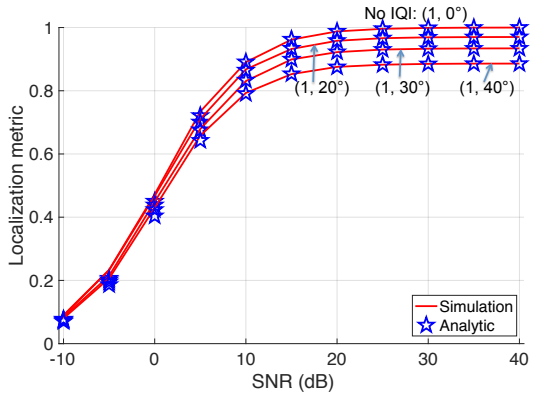


Fig. 4. Localization metric versus SNR for different phase imbalances. The couple $(\varepsilon, \theta)$ is noticed on each curve.

$\underline{\widetilde{H}}_{\mathcal{P}} = \underline{\underline{\Lambda}}_{X_{\mathcal{P}}}^{-1} \cdot \underline{R}_{\mathcal{P}}$ without any corruption from image pilot symbols.

The calculated CFR corresponding to subset $\mathcal{P}$ is then interpolated to compute the CFR associated with subset $\overline{\mathcal{P}}$, which is $\underline{\widetilde{H}}_{\overline{\mathcal{P}}}$. The IQI parameter $\alpha$ is derived by

$$\alpha = (1/Q_1) \cdot \mathrm{tr}\left\{ \left( \underline{\underline{\Lambda}}_{\widetilde{H}_{\overline{\mathcal{P}}}} \cdot \underline{\underline{\Lambda}}_{\widetilde{X}_{\overline{\mathcal{P}}}} \right)^{-1} \underline{\underline{\Lambda}}_{R_{\overline{\mathcal{P}}}} \right\} \quad (8)$$

where $Q_1$ is the total number of inactive subcarriers indexes. From (1), it is easy to show that $\nu = 1 - \mu^*$ and from the definition of $\alpha$, we can derive the IQI parameters as follows (the detail derivation is skipped due to space constraint)

$$\mu = \frac{\Re(\alpha) - 1 - j\Im(\alpha)}{|\alpha|^2 - 1}, \quad \nu = \frac{|\alpha|^2 - \Re(\alpha) - j\Im(\alpha)}{|\alpha|^2 - 1} \quad (9)$$

The CFR can finally be estimated by $\underline{\widehat{H}} = 1/\mu \cdot \underline{\widetilde{H}}$.

## V. Results and Discussion

- *Channel model*:

A multi-path channel of type Extended Pedestrian A (EPA) [8] is used in simulations. Its power delay profile (PDP) is given in Table I. The overall channel power is normalized to unity for each channel realization. Each channel tap is assumed to be statistically independent from one to another.

TABLE I
PDP of the Extended Pedestrian A (EPA) channel.

| Excess tap delay (ns) | Relative power (dB) |
|---|---|
| 0 | 0.0 |
| 30 | -1.0 |
| 70 | -2.0 |
| 90 | -3.0 |
| 110 | -8.0 |
| 190 | -17.2 |
| 410 | -20.8 |

- *Validation of the derived localization metric*:

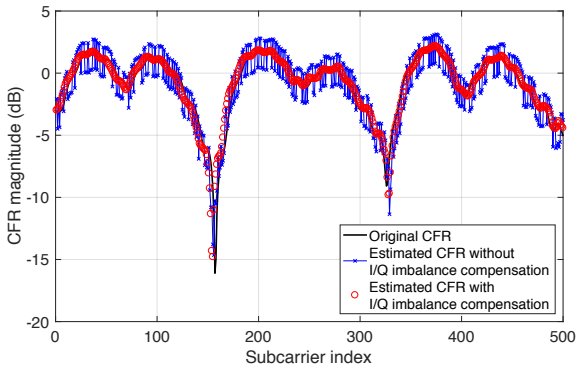


Fig. 5. Example of estimated CFR with and without IQI compensation, when $(\varepsilon, \theta) = (2, 10°)$ and SNR = 15 dB.

We consider a 512-subcarrier OFDM system, i.e., $Q = 512$. In order to focus on the IQI impact, the synchronization at the receiver side is assumed to be perfect. For each value of the signal-to-noise ratio (SNR), 1000 noise realizations are carried out to calculate the average value of localization metric. The numerical and analytical results are presented by the solid (or dashed) lines and marker symbols, respectively.

Figures 3 and 4 present the average localization metric values as a function of the different received SNR values for different gain and phase imbalances, respectively. In both figures, the analytical results match numerical ones, confirming the correctness of our derivation. Under the impact of IQI, the localization metric reduces, leading to the reduction of TR focusing gain and hence the reduction of the localization accuracy [4]. Intuitively, it can be explained by the fact that the CFR under the impact of IQI makes it different to the original one. At high SNRs, the localization metric converges asymtotically to a value. At low SNRs, suprisingly the localization metric with the gain imbalance (Fig. 3) is slightly bigger than that without IQI. It is due to the estimated CFR magnitude strongly varies under the gain imbalance impact (as seen later in Fig. 5),

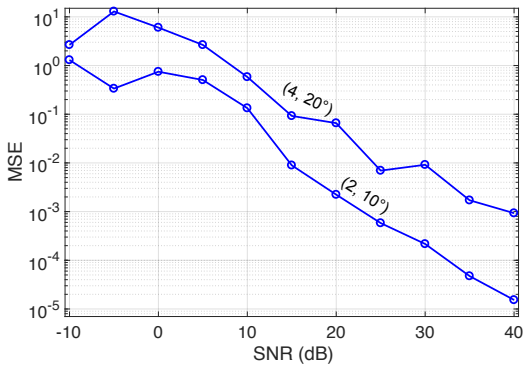


Fig. 6. MSE of estimated IQI parameter $\mu$ versus SNRs. The couple $(\varepsilon, \theta)$ is noticed on each curve.

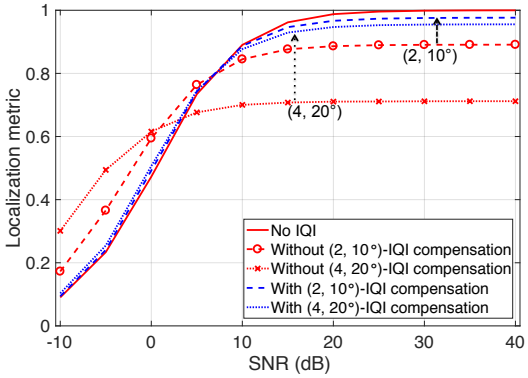


Fig. 7. Localization metric versus SNRs without and with IQI compensation. The couple $(\varepsilon, \theta)$ is noticed on each curve.

making the chance of constructive combination with the high AWGN bigger (i.e., becoming more similar to the original CFR), compared to the case of no IQI, which has only destructive AWGN effect within the CFR estimation. However, the localization metric value at low SNRs is small ($\leq 0.6$).

- *Validation of the proposed IQI compensation*:

Figure 5 presents the estimated CFRs when $(\varepsilon, \theta) = (2, 10°)$ and SNR = 15 dB. It is clearly seen that without IQI compensation, the estimated CFR using conventional pilot symbols strongly varies compared to the original one, while with the proposed IQI compensation, the estimated CFR is similar to the original one.

To verify the effectiveness of proposed IQI compensation, we calculated the mean-square-error (MSE) of the estimated IQI parameter $\mu$ as a function of SNRs (Fig. 6). It can be observed that MSE gradually improves with the increase of SNR. Thanks to the designed pilots, the estimated $\mu$ is disrupted only by the AWGN and not by the image-pilots. The IQI estimation can be improved further by using a bigger number of subcarriers or averaging over more OFDM symbols.

Finally, we investigate the localization metric improvement after the IQI compensation. Fig. 7 presents the localization metric as a functions of SNR with and without IQI compensation. It is clearly seen that even with the strong IQI values, i.e., $(\varepsilon, \theta) = (4, 20°)$, the localization metric can be brought back close to the one without IQI thanks to the proposed designed pilots. Consequently, TRIPS system can mitigate the positioning estimation error inherent to the IQI and hence improve the failure ratio of the positioning estimation [4].

## VI. Conclusion

We have studied the impact of IQI in the time-reversal based indoor positioning systems (TRIPS). We have derived a closed-form expression of the localization metric in the presence of the IQI. The results showed that compared to the case of no IQI, the localization metric of TRIPS reduces in the presence of the IQI, leading to the increase of the positioning error. An efficient IQI compensation has been proposed and validated. It is shown that thanks to the IQI compensation, the localization metric values are brought back to the one in the case of no IQI, confirming the effectiveness of our proposed IQI compensation.

## Appendix A

- *Numerator derivation of* (5): $T_1 = \mathbb{E}\left[\left|\underline{H}^H \cdot \underline{\widehat{G}}\right|^2\right]$

Applying the law of total expectation, $T_1$ can be rewritten as

$$T_1 = \mathbb{E}_H\left[\mathbb{E}_{W|H}\left[\left|\underline{H}^H \cdot \underline{\widehat{G}}\right|^2 \middle| \underline{H}\right]\right] \tag{10}$$

The inner expectation $E_1 = \mathbb{E}_{W|H}\left[\left|\underline{H}^H \cdot \underline{\widehat{G}}\right|^2 \middle| \underline{H}\right]$ can be further manipulated as follows

$$\begin{aligned} E_1 = {} & \mathbb{E}_{W|H}\left[\left|\sum_{q=0}^{Q-1}(\mu + \nu Z_q)\cdot|H_q|^2\right|^2 \middle| \underline{H}\right] \\ & + \mathbb{E}_{W|H}\left[\left|\sum_{q=0}^{Q-1}\frac{H_q^*}{X_q}\cdot W_q\right|^2 \middle| \underline{H}\right] \\ & + 2\mathbb{E}_{W|H}\left[\Re\left\{\sum_{p=0}^{Q-1}(\mu + \nu Z_p)\,|H_p|^2 \right.\right. \\ & \left.\left. \cdot \sum_{q=0}^{Q-1}\frac{H_q^*}{X_q}\cdot W_q\right\} \middle| \underline{H}\right] \end{aligned} \tag{11}$$

The third term of (11) is equal to 0, as $\mathbb{E}[\Re\{W_q\}] = 0$. We can straightforwardly derive $E_1$ as follows

$$E_1 = \left|\sum_{q=0}^{Q-1}(\mu + \nu Z_q)\,|H_q|^2\right|^2 + \sum_{q=0}^{Q-1}|H_q|^2\sigma_W^2 \tag{12}$$

Due to the fact that the random variable (RV) $|H_q|^2$ has the probability density function (PDF) $f_X(x) =$

$\mathrm{e}^{-x}$ [9] and $\mathbb{E}[|H_q|^2] = 1$, substituting (12) into $T_1$, then $T_1$ can be rewritten as $T_1 = E_2 + Q \cdot \sigma_W^2$, where $E_2 = \mathbb{E}_H \left[ \left| \sum_{q=0}^{Q-1} (\mu + \nu Z_q) |H_q|^2 \right|^2 \right]$ can be expressed as

$$E_2 = \sum_{p=0}^{Q-1} \sum_{q=0}^{Q-1} (\mu + \nu Z_p)(\mu + \nu Z_q)^* \mathbb{E}_H \left[ |H_p|^2 |H_q|^2 \right] \tag{13}$$

We now derive $E_3 = \mathbb{E}_H \left[ |H_p|^2 |H_q|^2 \right]$. Applying again the law of total expectation, $E_3$ is rewritten as

$$\begin{aligned} E_3 &= \mathbb{E}_{H_q} \left[ \mathbb{E}_{H_p|H_q} \left[ |H_p|^2 |H_q|^2 \middle| H_q \right] \right] \\ &= \mathbb{E}_{H_q} \left[ |H_q|^2 \cdot \mathbb{E}_{H_p|H_q} \left[ |H_p|^2 \middle| H_q \right] \right] \end{aligned} \tag{14}$$

As CFR components are correlated, the conditional expectation and co-variance can be derived based on results in [10]: $\mathbb{E}_{H_p|H_q}[H_p| H_q] = \rho_{q-p} \cdot H_q$ and $\mathrm{Cov}(H_p| H_q) = 1 - |\rho_{q-p}|^2$, for $\forall p, q = 0, ..., Q-1$, where $\rho_{q-p}$ is the correlation between $H_p$ and $H_q$ derived in Appendix B. The inner expectation of (14) $E_4 = \mathbb{E}_{H_p|H_q} \left[ |H_p|^2 \middle| H_q \right]$ is derived by [10]

$$\begin{aligned} E_4 &= \mathrm{Cov}(H_p| H_q) \\ &\quad + \mathbb{E}_{H_p|H_q}[H_p| H_q] \cdot \left( \mathbb{E}_{H_p|H_q}[H_p| H_q] \right)^H \\ &= 1 - |\rho_{q-p}|^2 + |\rho_{q-p}|^2 |H_q|^2 \end{aligned} \tag{15}$$

Substituting (15) into (14) and taking the fact that $\mathbb{E}\left[|H_q|^4\right] = \int_0^\infty x^2 \cdot \mathrm{e}^{-x} dx = \Gamma(3) = 2$, where $\Gamma(\cdot)$ is the Gamma function, we can derive $E_3 = 1 + |\rho_{q-p}|^2 := \Theta_{pq}$. Finally, substituting the derived $E_1$, $E_2$ and $E_3$ into $T_1$, we obtain the derived numerator of (5) as in (6).

- *Denominator derivation of* (5): $T_2 = \mathbb{E}\left[ \|\underline{H}\|_2^2 \cdot \left\| \widehat{\underline{G}} \right\|_2^2 \right]$

Similar to the derivation of $T_1$, we first re-write $T_2$ using the law of total expectation: $T_2 = \mathbb{E}_H \left[ \mathbb{E}_{W|H} \left[ \|\underline{H}\|_2^2 \cdot \left\| \widehat{\underline{G}} \right\|_2^2 \middle| \underline{H} \right] \right]$. We then compute the inner expectation in the $T_2$ expression: $F_1 = \mathbb{E}_{W|H} \left[ \|\underline{H}\|_2^2 \cdot \left\| \widehat{\underline{G}} \right\|_2^2 \middle| \underline{H} \right]$, which is derived as follows

$$\begin{aligned} F_1 &= \mathbb{E}_{W|H} \left[ \sum_{p=0}^{Q-1} |H_p|^2 \right. \\ &\qquad \left. \cdot \sum_{q=0}^{Q-1} \left| (\mu + \nu Z_q) H_q + \frac{W_q}{X_q} \right|^2 \middle| \underline{H} \right] \\ &= Q\sigma_W^2 \sum_{p=0}^{Q-1} |H_p|^2 + \sum_{p=0}^{Q-1} \sum_{q=0}^{Q-1} |\mu + \nu Z_q|^2 |H_p|^2 |H_q|^2 \end{aligned} \tag{16}$$

Substituting the previous derived expection $\mathbb{E}\left[ |H_p|^2 |H_q|^2 \right] = \Theta_{pq} := 1 + |\rho_{q-p}|^2$ and the fact that $\mathbb{E}[|H_p|^2] = 1$ into (16), we can obtain the derived denominator of (5) as in (6).

## APPENDIX B

Considering a $L$-tap channel impulse response (CIR) $\underline{h}$ of the $l$-th tap variance: $\sigma_{h_l}^2 = \mathbb{E}\left[ |h_l|^2 \right]$ and assuming that the CIR taps are independent from one to another, i.e., $\mathbb{E}[h_l h_m^*] = 0$ for $\forall l \neq m$, the $p$-th and $q$-th CFR components are $H_p = 1/\sqrt{Q} \sum_{l=0}^{L-1} h_l \cdot \exp(-j2\pi lp/Q)$ and $H_q = 1/\sqrt{Q} \sum_{m=0}^{L-1} h_m \cdot \exp(-j2\pi mq/Q)$, respectively. The CFR correlation between the $p$-th and $q$-th compents is derived as follows

$$\begin{aligned} \rho_{q-p} &= \mathbb{E}\left[ H_p H_q^* \right] \\ &= \frac{1}{Q} \sum_{l=0}^{L-1} \sum_{m=0}^{L-1} \mathbb{E}[h_l h_m^*] \cdot \mathrm{e}^{j2\pi(mq-lp)/Q} \\ &= \frac{1}{Q} \sum_{l=0}^{L-1} \sigma_{h_l}^2 \cdot \mathrm{e}^{j2\pi l(q-p)/Q} \end{aligned} \tag{17}$$


## ACKNOWLEDGMENT

The authors would like to thank the financial supports of the Copine-IoT Innoviris project, the Icity.Brussels project and the FEDER/EFRO grant.


## REFERENCES


[1] J. Xiao, K. S. Wu, Y. Yi, and L. M. Ni, "FIFS: Fine-grained indoor fingerprinting system," 21st Int. Conf. on Computer Commun. and Netw. (ICCCN), pp. 1–7, Jul. 2012.

[2] Z.-H. Wu, Y. Han, Y. Chen, and K. J. R. Liu, "A time-reversal paradigm for indoor positioning system," IEEE Trans. Veh. Technol., vol. 64, no. 4, pp. 1331–1339, Apr. 2015.

[3] F. Horlin, A. Bourdoux, and L. Van der Perre, "Low-complexity EM-based joint acquisition of the carrier frequency offset and IQ imbalance," IEEE Trans. Wireless Commun., vol. 7, no. 6, pp. 2212–2220, Jun. 2008.

[4] T.-H. Nguyen, J. Louveaux, P. De Doncker, and F. Horlin, "Impact of I/Q imbalance on time reversal-based indoor positioning systems," 14th Int. Conf. on Wireless and Mobile Computing, Netw. and Commun. (WiMob), pp. 36–41, Limassol, Cyprus, Oct. 2012.

[5] T. Schenk, "RF imperfections in high-rate wireless systems: Impact and digital compensation," Springer publisher, 1st ed., 2008.

[6] C. Chen, Y. Han, Y. Chen, and K. J. R. Liu, "Indoor global positioning system with centimeter accuracy using Wi-Fi," IEEE Signal Processing Magazine, vol. 33, no. 6, pp. 128–134, Nov. 2016.

[7] Y.-H. Chung, and S.-M. Phoong, "Channel estimation in the presence of transmitter and receiver I/Q mismatches for OFDM systems," IEEE Trans. Wireless Commun., vol. 8, no. 9, pp. 4476–4479, Sep. 2009.

[8] 3GPP - TS 36.101, "User Equipment (UE) Radio Transmission and Reception." 3rd Generation Partnership Project; Technical Specification Group Radio Access Network; Evolved Universal Terrestrial Radio Access (E-UTRA). URL: http://www.3gpp.org.

[9] A. Papoulis, "Probability, random variables and stochastic processes," McGraw-Hill Companies, 3rd edition, 1991.

[10] S. M. Kay, "Fundamental of statistical signal processing: Estimation theory," Prentice Hall, 1st edition, 1993.